



Research Report

Memory Effect in a Lithium-ion Battery

Tsuyoshi Sasaki, Yoshio Ukyo and Petr Novák

Report received on Jul. 10, 2014

■ABSTRACT■ So-called ‘memory effects’ are well known to users of nickel-cadmium and nickel-metal-hydride batteries. If these batteries are recharged repeatedly after being only partially discharged, they gradually lose usable capacity due to a reduced working voltage. Lithium-ion batteries, in contrast, are considered to have no memory effect. Here we report a clear memory effect of LiFePO_4 – one of the materials used for the positive electrode in Li-ion batteries – that appears already after only one cycle of partial charge and discharge. We characterize this memory effect of LiFePO_4 and explain its connection to the so-called particle-by-particle charge/discharge model. Not least with a view to practical use of Li-ion batteries in automobiles, this tiny memory effect is important for a majority of battery uses, as the slight voltage change it causes can lead to substantial mistakes in estimating the state of charge of the batteries.

■KEYWORDS■ Lithium-ion, Battery, Memory Effect, State of Charge, Charge/discharge, LiFePO_4 , Two-phase System

1. Introduction

Lithium-ion batteries (LIBs) are the state-of-the-art power sources for mobile phones, laptops, and electronic devices. Furthermore, LIBs have now emerged as the most promising power source for electric vehicles, hybrid vehicles, and plug-in hybrid vehicles. Relative to alternative systems such as nickel-cadmium (Ni–Cd) or nickel-metal-hydride (Ni–MH) batteries, LIBs offer several advantages, including smaller size and lower weight. Moreover, LIBs are considered to have no memory effect.⁽¹⁻³⁾ Whereas the term memory effect may be known mainly to specialists, its consequences are familiar to many, in the form of reduced available service time of a shaver or a mobile power tool. In Ni–Cd and Ni–MH batteries, the memory effect is manifested in a reduced working voltage, which is observed in the discharge curves when the batteries undergo repeated shallow-depth discharge for a large number of cycles⁽³⁻⁷⁾ – the discharge voltage seems to memorize the depth of discharge of the previous cycling. This memory effect leads to a reduction in practical cell capacity at a fixed cut-off voltage and/or to a wrong estimate of the state

of charge (SOC) of the cell. This is problematic in particular for batteries used in automobiles.^(8,9)

The belief that LIBs have no memory effect prevails since they have been commercialized in the early of 1990s.⁽¹⁻³⁾ (In this paper, we reserve the term ‘memory effect’ for abnormal changes in working voltage – as in the examples above – which does not include hysteresis behaviour during charge and discharge.) One paper⁽¹⁰⁾ reported, in 1991, memory-effect-like behaviour of electrolytic manganese dioxide (EMD) for Li-metal batteries, but not for Li-ion batteries. To our knowledge, there has been no dedicated study that tried to confirm the absence of a memory effect in LIBs. In preparation for the commercialization of electric, hybrid, and plug-in hybrid vehicles, revisiting the question whether LIBs exhibit memory effects or not is therefore called for.

In the following, we focus on the occurrence of memory effects of LiFePO_4 ^(11,12) and $\text{Li}_4\text{Ti}_5\text{O}_{12}$.^(13,14) There are two reasons for choosing these particular materials. First, LiFePO_4 and $\text{Li}_4\text{Ti}_5\text{O}_{12}$ are rather safe and inexpensive materials for LIBs, compared to other candidates, such as LiCoO_2 and $\text{Li}(\text{Ni}, \text{Co}, \text{Al})\text{O}_2$.^(12,15-17) These characteristics are essential for the use in automobiles. Second, the charge/discharge voltage curves of these materials are very flat, as they undergo a two-phase reaction.^(11,14) Therefore, a small anomalous voltage change should account for a large mis-estimate

Reprinted from Nature Materials, Vol. 12, pp. 569-575
(<http://dx.doi.org/10.1038/NMAT3623>), © 2013 Macmillan Publishers Limited, with permission from Nature Publishing Group.

of the SOC. Consequently, even small memory effects would lead, if they remain unidentified, to considerable practical problems for LIBs based on LiFePO_4 or $\text{Li}_4\text{Ti}_5\text{O}_{12}$.

2. Memory Effect of LiFePO_4

To our surprise, we found a clear memory effect in the charge curve of LiFePO_4 . Moreover, the phenomenon is seen already after a single cycle of shallow-depth charge and discharge. **Figure 1** shows a typical example of the memory effect of LiFePO_4 at a SOC of 50% at about $C/2$ rate. (A rate of C/n corresponds to a full charge or discharge in n h.) A normal charge/discharge curve of LiFePO_4 between 2.4 and 4.4 V is shown in Fig. 1(a). The procedure for checking whether the memory effect occurs is shown in Fig. 1(c). After the first partial cycle, a small bump suddenly appeared at a SOC of 50% in the charge curve of the subsequent

cycle of full charge and discharge (Fig. 1(d), red line). After a further cycle of full charge and discharge, the small bump completely disappeared (Fig. 1(d), black line). We define the partial charge/discharge cycle as a memory-writing cycle, and the subsequent full cycle as a memory-releasing cycle. To our knowledge, this is the first report of a memory effect in materials for Li-ion batteries.

The SOC where the small bump appears clearly depends on the depth of charge and discharge of the previous cycle, as shown in **Fig. 2**. Each memory-writing cycle included a rest time of one hour between charge and discharge in the open-circuit state. The rest time between the memory-writing cycle and the memory-releasing cycle was 10 minutes. The charge-voltage curves in the memory-releasing cycles seem to recall the depth of the previous cycle, even after full discharge. Although the memory effect is rather small, the slight voltage change will still lead

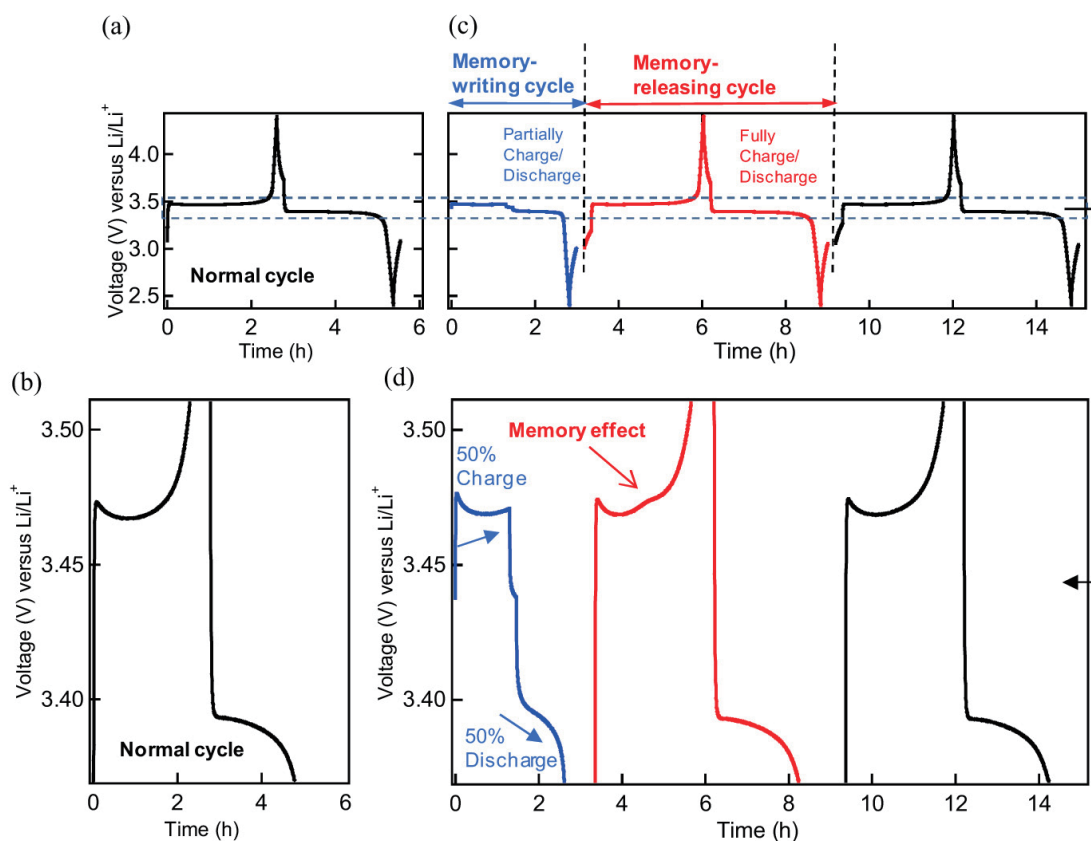


Fig. 1 Demonstration of a memory effect in LiFePO_4 at a SOC of 50%. (a) Normal charge and discharge curve between 2.4 and 4.4 V vs. Li/Li^+ . (b) Enlarged view of Fig. 1(a) between 3.45 and 3.50 V. (c) A sequence of three cycles. First cycle (blue line): charge up to a SOC of 50% and full discharge until 2.4 V; second (red line) and third cycle (black line): full charge and discharge between 2.4 and 4.4 V. (d) Enlarged view of Fig. 1(c) between 3.45 and 3.50 V. The charge/discharge current rate is $C/2$. The red arrow in Fig. 1(d) shows a typical memory effect at SOC 50%.

to a significantly inaccurate estimate of the SOC of the LIB, as the charge/discharge curve of LiFePO_4 is very flat over a wide region. Of course, the voltage of an entire battery is determined by the difference between the electrochemical potentials of the positive and negative electrode. If the negative electrode has a sloped charge/discharge curve, that would be helpful to accurately estimate the SOC. However, the most popular negative-electrode materials for LIBs, graphite and $\text{Li}_4\text{Ti}_5\text{O}_{12}$, have wide flat regions in their charge/discharge curves.^(13,14,18,19) These systems will suffer from the memory effect due to the flatness of its battery voltage. For the SOC estimations, the Coulomb-counting method⁽²⁰⁾ can be used, however the method is not suitable for LIBs in automobile uses.⁽²¹⁾ LIBs always have some side reactions that lead to irreversible capacity, self-discharge, and degradation,^(20,21) especially at elevated temperatures; also, the required accuracy of the SOC is particularly high for automobile uses.⁽²²⁾

The new memory effect has the following characteristics. First, the memory is not erased after full discharge with constant current up to 2.4 V; however, the memory is completely erased after full charge at the same current rate. Second, in contrast to Ni–Cd and Ni–MH batteries, in LiFePO_4 the memory effect appears already after only one partial cycle. The effect of repeating the memory-writing cycle is shown in Supplementary Information S1. Increasing the number of repetitions of the memory-writing cycle to the same SOC made the memory effect more pronounced. The rate dependency of the memory-releasing cycle is shown in Supplementary Information S2. The memory

effect was found even at higher rates of 1C and 4C. The height of the memory bumps seems to increase with higher rates, suggesting that the memory effect seem to act as a resistance. In the case of discharge processes, the memory effect of LiFePO_4 was much smaller, but it still existed, as shown in **Figs. 3(a)** and **(b)**. To provide further evidence of the memory effect, we confirmed it in a number of other setting: in three-electrode cells as shown in Supplementary Information S3; with very thin electrodes (less than 4% loading compared with the standard electrodes used in this study) as shown in Supplementary Information S4; and with different rates of memory-writing and memory-releasing cycles as shown in Supplementary Information S5. In all of these configurations, the memory effect was detected. These results suggest that the effects of the cell-configuration, electrode-structure, and rate settings are not critical factors for the memory effect in LiFePO_4 .

The memory effect seems to be more involved and far-reaching (with a view to practical uses of LIBs) than hysteretic effects during charging and discharge. It is known that some active materials for LIBs exhibit hysteresis even in very slow C rates.⁽²³⁾ The hysteresis can be regarded as a kind of memory of the most recent history. However the memory effect described here has dependencies beyond the most recent history. An example is shown in Supplementary Information S1, where the memory bump is growing in size with an increasing number of repetitions of the memory-writing cycle. Figure 2 shows another example to confirm the dependency on the history. The most recent histories just before the memory-releasing

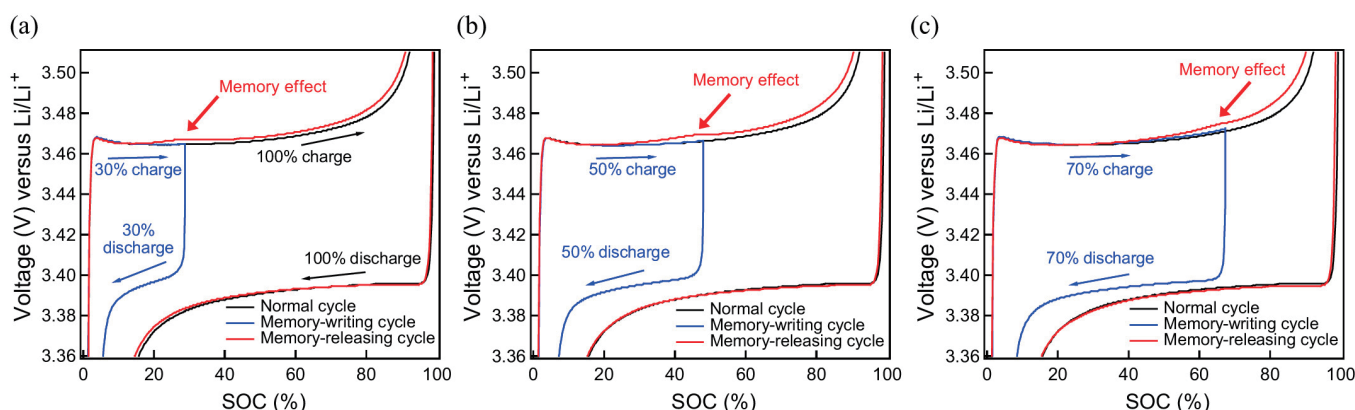


Fig. 2 The memory effect in LiFePO_4 at several SOC. (a) SOC 30%. (b) SOC 50%. (c) SOC 70%. Black, blue, and red lines correspond to normal cycle, memory-writing cycle, and memory-releasing cycle, respectively.

cycles were identical in the conditions of Fig. 2(a) to (c); however, the subsequent memory-releasing cycles showed clear dependencies beyond the most recent history.

To gain mechanistic insight into the memory effect of LiFePO_4 , it is helpful to compare it with the behaviour of $\text{Li}_4\text{Ti}_5\text{O}_{12}$, as both materials undergo a two-phase reaction.^(11,14) Figures 3(c) and (d) show the charge/discharge curve of $\text{Li}_4\text{Ti}_5\text{O}_{12}$ cells for the same procedure that was used in the experiments shown in Figs. 3(a) and (b). In contrast to LiFePO_4 , $\text{Li}_4\text{Ti}_5\text{O}_{12}$ showed no detectable memory effect. This result is important from two perspectives. First, the observed behaviour of $\text{Li}_4\text{Ti}_5\text{O}_{12}$ cells supports the notion that the memory effect seen in LiFePO_4 cells is not due to any of the other components – Li-metal counter electrode, conductive carbon, binder, electrolyte, and so on – because the component materials in the $\text{Li}_4\text{Ti}_5\text{O}_{12}$ cells were identical to those in the LiFePO_4 cells. Second, the two-phase reaction itself is not a sufficient condition for the memory effect. Therefore, the key to understanding the mechanism of the memory

effect should be in the different behaviours of LiFePO_4 and $\text{Li}_4\text{Ti}_5\text{O}_{12}$.

To examine the electrochemical differences between LiFePO_4 and $\text{Li}_4\text{Ti}_5\text{O}_{12}$, we conducted galvanostatic intermittent titration technique (GITT) measurements⁽²⁴⁾ for both materials. As a reference, constant current (CC) measurements were conducted using the same cells, at the same $C/2$ current rate. **Figure 4** shows the result of the GITT measurements, superimposed with the result of CC measurements. The flat open-circuit voltage (OCV), as shown by red lines in Fig. 4, is expected, as the two-phase reaction happens in the flat region. A notable feature is the difference of the polarizations between the CC measurement and the closed-circuit voltage (CCV) in the GITT measurement, as marked X in Fig. 4(a). As the same $C/2$ current rate was applied in both the CC and the GITT measurements, the polarization should be identical, especially in the case of active materials with two-phase reaction. In fact, the first step of CCV in GITT (black line) was essentially identical to the CC measurement (blue line), as shown in Figs. 4(a) and

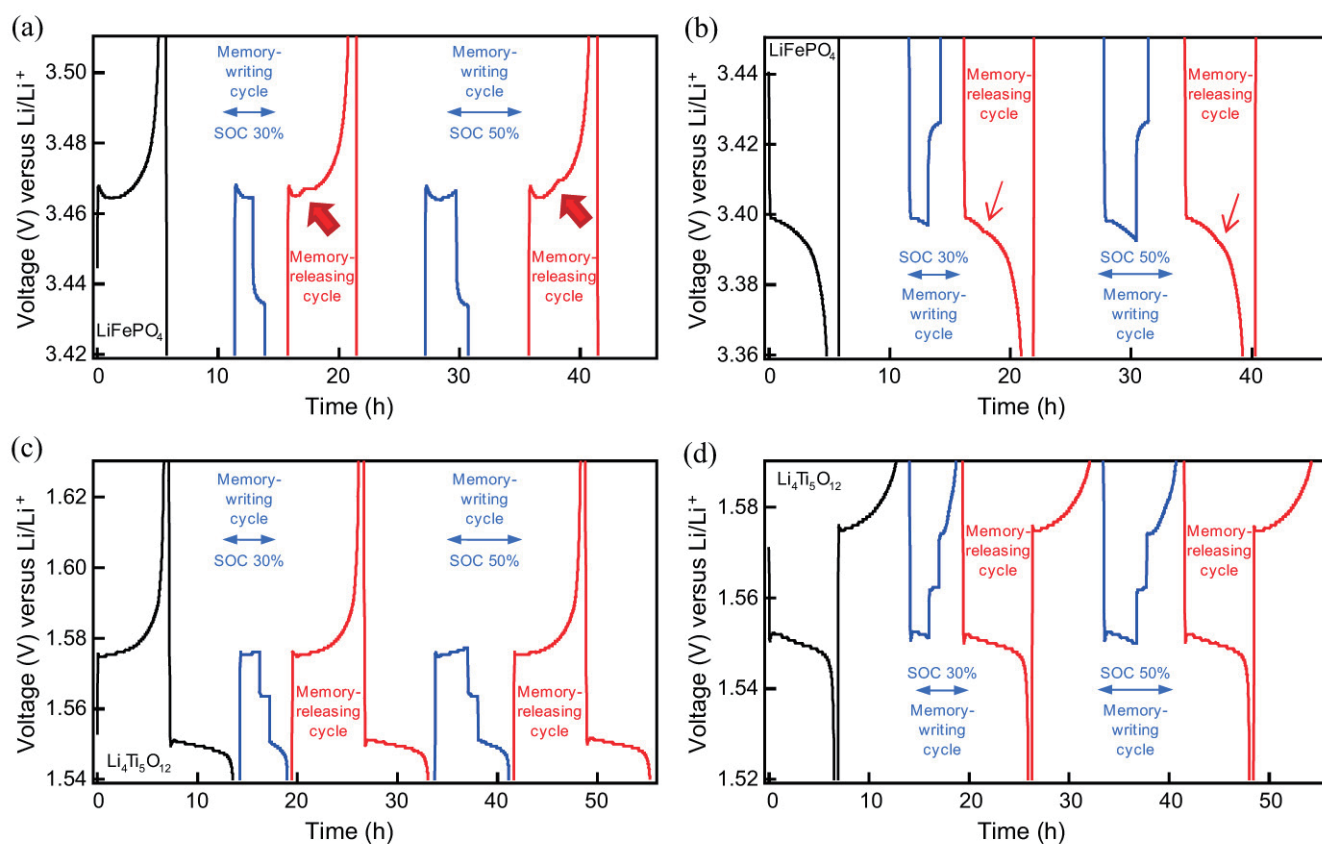


Fig. 3 Charge and discharge curve of LiFePO_4 and $\text{Li}_4\text{Ti}_5\text{O}_{12}$ under ‘memory-effect conditions’ at SOC of 30% and 50%. (a) (b) Charge (a) and discharge (b) process of LiFePO_4 . (c) (d) Charge (c) and discharge (d) process of $\text{Li}_4\text{Ti}_5\text{O}_{12}$.

(b). However, the two polarizations showed significant differences, starting from the second charge/discharge cycle. On the other hand, the two polarizations – the CCV in GITT measurements and the voltage curves in CC measurements – were identical in the case of $\text{Li}_4\text{Ti}_5\text{O}_{12}$, as shown in Figs. 4(c) and (d). This suggests a difference in the electrochemical behaviour of $\text{Li}_4\text{Ti}_5\text{O}_{12}$ and LiFePO_4 . In brief, $\text{Li}_4\text{Ti}_5\text{O}_{12}$ exhibited normal behaviour, whereas LiFePO_4 showed an anomalous polarization increase after relaxation in the GITT measurements.

A further notable observation relates to the beginning of the charge and discharge curves of the two active materials in both GITT and CC measurements. In the LiFePO_4 charge process, a distinct overshoot was

found, marked Y in Fig. 4(a). Also in the discharge process of LiFePO_4 and in the charge/discharge process of $\text{Li}_4\text{Ti}_5\text{O}_{12}$, slight initial overshoots were found. This effect should be due to kinetics effect, as none of the OCV curves shows such a bump. This type of overshoot at the beginning of charge curves can be seen as well in other published data on LiFePO_4 .⁽²⁵⁻²⁹⁾ These two features, marked in Fig. 4(a) as X and Y, are the keys to understanding the mechanism of the observed memory effect.

3. Model of the Memory Effect of LiFePO_4

To explain the X feature seen in the GITT measurements (Fig. 4(a)), we checked a wide range of

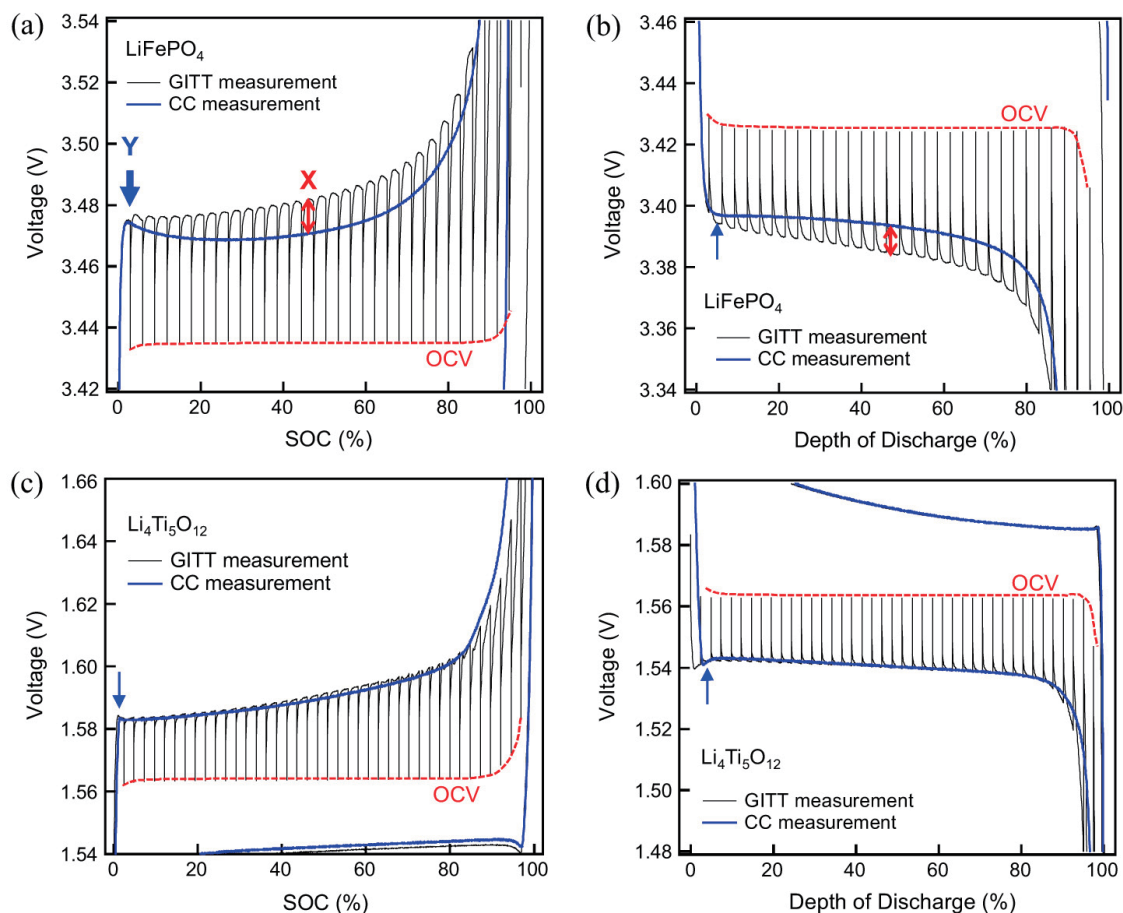


Fig. 4 GITT and constant current measurements of LiFePO_4 and $\text{Li}_4\text{Ti}_5\text{O}_{12}$ between 2.4 and 4.4 V vs. Li/Li^+ for LiFePO_4 and 1.0 and 2.1 V for $\text{Li}_4\text{Ti}_5\text{O}_{12}$, respectively. Black and blue lines correspond to GITT and CC measurements, respectively. The GITT measurements consist of a series of current pulses applied at $C/2$, each followed by a 2-h relaxation period. The red dashed line shows the OCV curve, constructed by connecting the voltage points after each relaxation period. The current rate of the CC measurement was also $C/2$. (a) (b) Charge (a) and discharge (b) process of LiFePO_4 . (c) (d) Charge (c) and discharge (d) process of $\text{Li}_4\text{Ti}_5\text{O}_{12}$.

charge/discharge models for LiFePO_4 . These models include the core-shell model,⁽¹¹⁾ the mosaic model,⁽³⁰⁾ the radial core-shell model,⁽³¹⁾ the spinodal-decomposition model,⁽³²⁾ and the domino-cascade model,⁽³³⁾ However, these models cannot explain the mechanism of the memory effect. Recently, so-called many-particle models have been reported, which are based on a non-monotone single-particle chemical potential for LiFePO_4 .^(29,34) The many-particle model proposed in ref. (29) can explain the first feature (X) in the GITT measurement of LiFePO_4 . The model describes the possible shapes of the chemical potential of single LiFePO_4 particles in a solid solution, two-phase equilibrium, and the galvanostatic curve (Fig. 5(a)). The two-phase equilibrium potential is such that a Li-rich phase can coexist with a Li-poor phase. The galvanostatic curve refers to the simplified path in the case of phase separation controlled by a typical galvanostatic experiment under very slow charge/discharge rates.⁽²⁹⁾ The shape of the chemical potential for the solid solution is consistent with recent results obtained in Monte Carlo simulations.⁽³⁵⁾ The many-particle model suggests that discrete, one-by-one filling of many particles is responsible for the voltage plateaux in the charge/discharge voltage curves of LiFePO_4 . When we start from many fully discharged LiFePO_4 particles (Fig. 5(b)) and gradually decrease the Li mole fraction x of the particles by applying a charging current, then every particle can reach the vicinity of point B through homogeneous solid-state reactions. At point B, one or a few particles will undergo spinodal decomposition and become inhomogeneous by forming the two-phase system – composed of a Li-rich and a Li-poor phase – as indicated by the red arrow in Fig. 5(b). Most of the particles will still be in a homogeneous Li-rich phase when reaching point B. The particle that decomposed into two phases quickly moves towards point C, as indicated by the blue arrow in Fig. 5(b), to establish a homogeneous Li-poor phase by interactions with other surrounding Li-rich particles. In this reaction, another particle at point B, likely to be far away from the first charged particle, will undergo spinodal decomposition, and charging proceeds. The fate of a particle will be determined by slight differences in the electrochemical environment of the particles. This sequential particle-by-particle charging process creates a flat many-particle equilibrium potential as shown by the green line in Fig. 5(b).

Next we consider the behaviour seen in the GITT measurements in the light of the sequential particle-by-particle charging process. If the current is interrupted at a SOC of 30%, roughly 70% of the Li_xFePO_4 particles will still be in the Li-rich phase, and thus at point B of the chemical-potential curve (Fig. 5(c)). However, the system at point B is in an unstable state, and even if only a few particles will undergo spinodal decomposition, almost all other particles will go toward point A by exchanging lithium among each other and with particles in the Li-poor phase during relaxation (Fig. 5(c)). Figure 5(d) shows the state after relaxation. The particles are divided into two groups – roughly 70% Li-rich phase particles, and 30% Li-poor phase particles (Fig. 5(c)).

Now we can turn to the polarization difference seen between the CC measurement and the GITT measurements. Figures 5(c) and (d) show the charging condition in the CC and the GITT measurement, respectively. To proceed with charging from the condition shown in Fig. 5(d), the polarization should be larger than that in the condition of Fig. 5(c), as the Li-rich particles should climb again toward point B, which is at a higher chemical potential (see the dashed arrow in Fig. 5(d)). Moreover, the Li-rich particles – which are the active particles in the charging process – are reduced to a fraction of 70%, compared with the condition depicted in Fig. 5(b). To sum up, the many-particle model and the non-uniform chemical potential of LiFePO_4 can explain the polarization behaviour of the GITT measurements indicated by blue arrows in Figs. 4(a) and (b).

However, the origin of the overshoots at the beginning of charge and discharge curves – the behaviour indicated by arrows Y in Fig. 4 – is still unexplained. On close inspection, the overshooting can be observed in the each charging process recorded in the GITT measurement (Fig. 4(a)), where charging starts from the condition of Fig. 5(d). It is most likely that the overshoots are due to some resistance involved with the spinodal decomposition or nucleation formation between points A to B. The overshoots will appear just before the sequential particle-by-particle process takes place. That we start charging from the condition of Fig. 5(d), is the triggering condition of the overshooting.

Now we can explain the memory effect in the light of the many-particle model and the overshooting

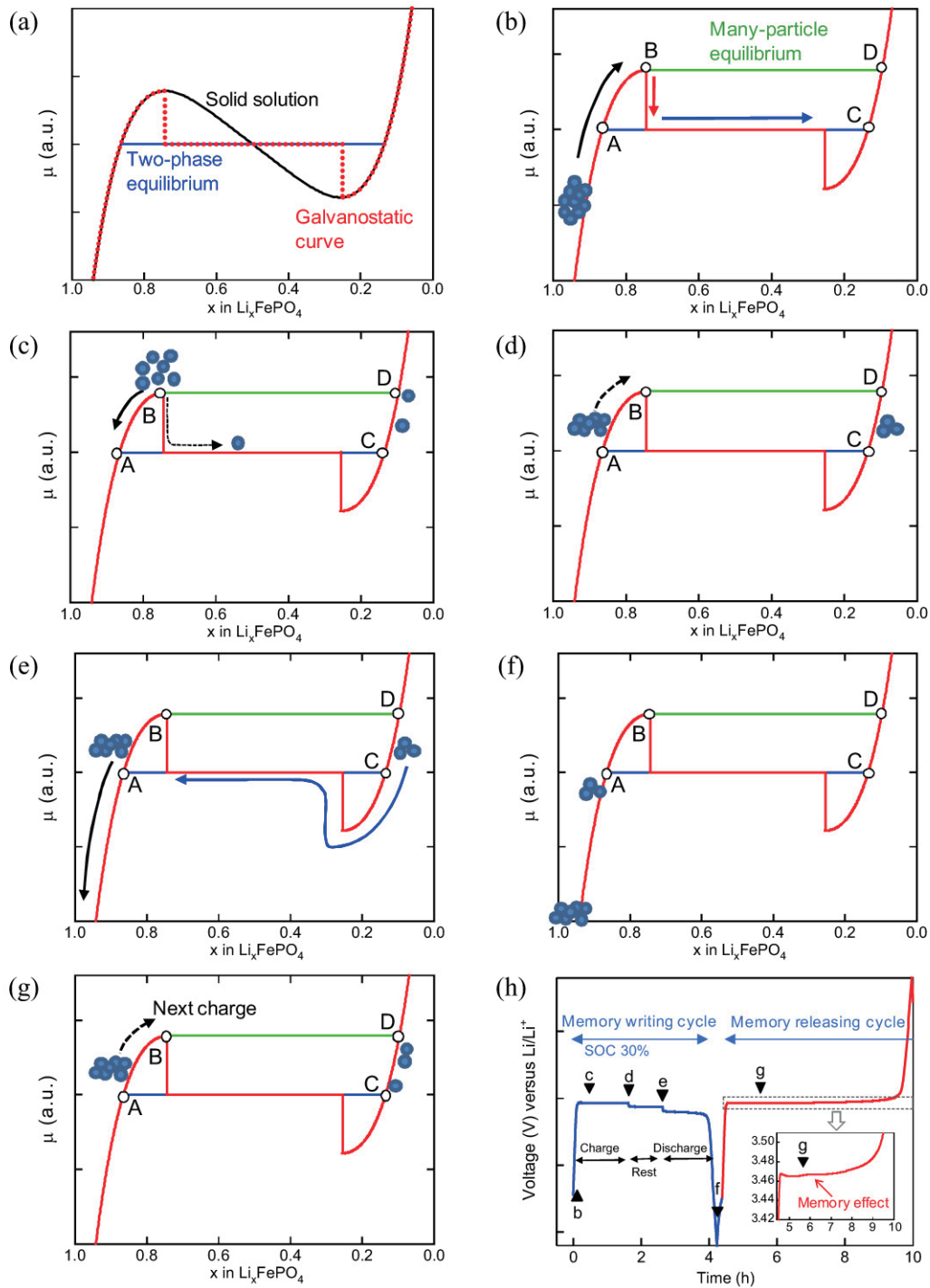


Fig. 5 Schematic diagram of the chemical-potential condition of many particles of LiFePO_4 during GITT measurement, the memory writing cycle, and the memory releasing cycle. (a) Possible shapes of the chemical potential of a single particle of LiFePO_4 for solid solution (black line), two-phase equilibrium (blue line), and the galvanostatic curve under very slow charge/discharge (red line).⁽²⁹⁾ (b) The initial condition at the beginning of the GITT measurement or the memory-writing cycle. The green line corresponds to the chemical potential of the many-particle equilibrium potential. (c) The condition during charging at a SOC of 30% in the GITT measurement or in the memory-writing cycle. (d) The condition after relaxation in the GITT measurement or in the memory-writing cycle at a SOC of 30%. (e) The condition at the beginning of discharge in the memory-writing cycle. (f) The condition at the end of discharge in the memory-writing cycle. (g) The condition just before the memory bump at a SOC of 30% in the memory-releasing cycle. (h) Diagram relating the conditions (b) to (g) to the memory-effect process.

phenomena. The conditions of Figs. 5(b) and (c) can be also used to explain the mechanism of the memory effect at a SOC of 30%. The relationship between the conditions and the process of the memory effect are shown in Fig. 5(h). Figure 5(e) shows the situation at the beginning of discharge in the memory-writing cycle at a SOC of 30%. The particles divide into two groups with distinctly different Li mole fraction; the ratio of the two groups is determined by the depth of the memory-writing cycle, in this case, 30% Li-poor phase particles and 70% Li-rich phase particles. Owing to the clear difference of Li mole fraction, even after discharge in the memory-writing cycle, the grouping will remain as shown in Fig. 5(e). The memory-releasing cycle then starts from the condition of Fig. 5(f). When the charge proceeds at a SOC of 30%, the first group will finish the sequential particle-by-particle charging as shown in Fig. 5(g). The second group has to go towards a higher chemical potential and thus will move toward point B. This situation is similar to the scenario of charging from the condition sketched in Fig. 5(d). Therefore, this is the triggering condition for the overshooting, as indicated in Fig. 4(a). To proceed with further charging, the overshoot will suddenly appear as the memory-effect bump. In other words, the memory bump will appear when the Li-rich particles climb up the chemical-potential curve toward point B without the sequential particle-by-particle charging situation. This suggests that the memory effect is expected to come from the delayed group, which is divided by the chemical-potential hill during the memory-writing cycle.

We conclude that the memory effect is the delayed overshooting, which normally appears at the beginning of the charge/discharge curve, owing to the division of the Li mole fraction into two groups, a Li-rich and a Li-poor phase. The relative population of the two groups is determined by the depth of the previous cycle, and the driving force of the division is the non-uniform chemical potential of LiFePO_4 . Both features seen in the GITT measurement (indicated by arrows X and Y in Fig. 4), are necessary for the memory effect to occur. Therefore, $\text{Li}_4\text{Ti}_5\text{O}_{12}$ shows no detectable memory effect and the memory effect in the discharge process of LiFePO_4 is much smaller.

We stress that our proposed mechanism is fundamentally different from that of the well-known memory effects observed in Ni–Cd and Ni–MH

batteries. In the case of Ni–Cd and Ni–MH batteries, the memory effect is due to a formation of an anomalous phase – HNi_2O_3 or $\gamma\text{-NiOOH}$ – by overcharging.^(6,7) Our model involves no anomalous phases and no overcharging.

To verify our model of the memory effect, we carried out several electrochemical experiments. The rest time between the memory-writing cycle and the memory-releasing cycle should be a critical factor. The separated particle groups at the end of the memory-writing cycle (see, for example, Fig. 5(f)), will reunite after long rest time, because of the gap in chemical potential. As expected, the memory effect disappeared when the rest time between the memory-writing cycle and the memory-releasing cycle is increased (Supplementary Information S6). The reunion of the separated groups by relaxation should work only at the end edge of the LiFePO_4 chemical potential.

When the two groups are separated before and after point B, the two groups never reunite, even after long rest time. To verify this expectation, we looked at the effect of the depth of discharge of the memory-writing cycle (see Supplementary Information S7). The rest time between the memory-writing cycle and the memory-releasing cycle was 10 min in all measurements. As shown in Supplementary Information S7, the memory effect was enhanced when decreasing the depth of discharge. This can be interpreted as deep discharge weakening the memory effect, owing to the potential gap and the reunion by relaxation during the 10-minute rest time. However, in the case of shallow-depth discharge, the reunion will not occur because of the chemical-potential hill to be overcome at point B.

Finally, we investigated the effect of the rest time after shallow-depth discharge in the memory-writing cycle (Supplementary Information S8). In contrast to the situation after full discharge (Supplementary Information S6), the memory effect did not disappear even after a rest time of 24 h, as predicted. These results (Supplementary Information S6 to 8) clearly support our model.

LiFePO_4 is one of the most promising positive electrode materials for automobile use and is used already in commercial LIBs. The memory effect described here should be taken into account especially for SOC estimations in LIBs with LiFePO_4 . We expect that the memory effect will occur not only in LiFePO_4

but also in other materials for LIBs as the proposed mechanism is quite universal for active materials with a non-monotone chemical potential. For example, LiMnPO_4 and LiNiPO_4 , which are other candidates for next-generation LIBs, should show this memory effect because they have the same olivine structure and two-phase reaction as LiFePO_4 . It is possible that some of the massive polyanion-type cathode materials⁽³⁶⁾ will show the memory effect as well, given that their structure and properties are similar to LiFePO_4 .

The small memory bump can have severe consequences on the durability and safety of industrial battery systems, due to the SOC mis-estimate by software algorithms. Nevertheless, the memory effect described here may be of practical use. In contrast to the memory effects in Ni-MH batteries, the memory effects in Li-ion batteries occur after only one partial charge/discharge cycle. It may therefore serve as a reliable indicator for estimating the SOCs of the Li-ion batteries. If some histories of the depth of the previous cycles are stored as a lookup table in the electrical control unit of the system, we can use the memory bump to estimate the SOCs.

4. Methods

The LiFePO_4 and $\text{Li}_4\text{Ti}_5\text{O}_{12}$ samples were provided by commercial suppliers, Nippon Chemical Industrial and Ishihara Sangyo Kaisha, respectively. All electrochemical tests were performed in standard two-electrode coin-type cells⁽³⁷⁾ or three-electrode cells (Toyo System), which feature a Li-metal reference electrode.⁽³⁸⁾ Li metal served as a counter electrode and glass-fiber separators were used. A 1 M solution of LiPF_6 in a 1:1 wt% mixture of ethylene carbonate and dimethyl carbonate was used as the electrolyte. The LiFePO_4 electrodes were prepared by casting the slurry, composed of 75 wt% active material, 10 wt% conductive carbon (TIMCAL Super-P), and 15 wt% polyvinylidene fluoride (PVdF; Solef 6020, Solvay SA) in the N-methyl-2-pyrrolidone solvent, on Al foil. The active material loading was approximately 5 mg cm^{-2} and the thickness of the coating layer was approximately $40 \text{ }\mu\text{m}$. The thin electrodes used for the experiments shown in Supplementary information S4 have been prepared by a spray technique. A spray nozzle produced 1 to $4 \text{ }\mu\text{m}$ thick electrodes with a load of 0.14 to 0.17 mg cm^{-2} of active material. The $\text{Li}_4\text{Ti}_5\text{O}_{12}$ electrodes were composed of 85 wt% active

material, 5 wt% conductive carbon, and 10 wt% PVdF. All coin-type test cells were electrochemically cycled three times before testing for the memory effect, between 2.4 and 4.4 V for LiFePO_4 electrodes and 1.0 and 2.1 V for $\text{Li}_4\text{Ti}_5\text{O}_{12}$ electrodes. All of the electrochemical measurements were conducted at $25 \pm 0.1 \text{ }^\circ\text{C}$ using an Astrol system (Astrol Electronics AG) or a VMP3 system (BioLogic) operating in galvanostatic mode.

End Notes

Supplementary Information is linked to the online version of the paper at www.nature.com/naturematerials.

Acknowledgements

We would like to thank C. Villevieille for experimental support and advice, M. Heß for helpful discussions and comments, S. Urbonaite for valuable suggestions on the manuscript and H. Kaiser and C. Junker for all-round technical assistance.

Author Contributions

T.S. conceived and carried out the experiments, analyzed the data and wrote the paper, Y.U. directed this work, P.N. discussed and directed this work.

References

- (1) Nishi, Y., "Lithium Ion Secondary Batteries; Past 10 Years and the Future", *J. Power Sources*, Vol.100, No. 1-2 (2001), pp. 101-106.
- (2) Pistoia, G., *Batteries for Portable Devices* (2005), Elsevier.
- (3) Vincent, C. A. and Scrosati, B., *Modern Batteries 2nd Edition* (1997), Elsevier.
- (4) Barnard, R., Crickmore, G. T., Lee, J. A. and Tye, F. L., "The Cause of Residual Capacity in Nickel Oxyhydroxide Electrodes", *J. Appl. Electrochem.*, Vol. 10, No. 1 (1980), pp. 61-70.
- (5) Davolio, G. and Soragni, E., "The 'Memory Effect' on Nickel Oxide Electrodes: Electrochemical and Mechanical Aspects", *J. Appl. Electrochem.*, Vol. 28, No. 12 (1998), pp. 1313-1319.
- (6) Huggins, R. A., "Mechanism of the Memory Effect in 'Nickel' Electrodes", *Solid State Ionics*, Vol. 177, No. 26-32 (2006), pp. 2643-2646.
- (7) Sato, Y., Takeuchi, S. and Kobayakawa, K., "Cause of

- the Memory Effect Observed in Alkaline Secondary Batteries using Nickel Electrode”, *J. Power Sources*, Vol. 93, No. 1-2 (2001), pp. 20-24.
- (8) Barbarisi, O., Vasca, F. and Glielmo, L., “State of Charge Kalman Filter Estimator for Automotive Batteries”, *Control Engineering Practice*, Vol. 14, No. 3 (2006), pp. 267-275.
- (9) Hu, Y. and Yurkovich, S., “Battery Cell State-of-charge Estimation Using Linear Parameter Varying System Techniques”, *J. Power Sources*, Vol. 198 (2012), pp. 338-350.
- (10) Sleigh, A. K., Murray, J. J. and Mckinnon, W. R., “Memory Effects due to Phase Conversion and Hysteresis in Li/Li_xMnO₂ Cells”, *Electrochim. Acta*, Vol. 36, No. 9 (1991), pp. 1469-1474.
- (11) Padhi, A. K., Najundaswamy, K. S. and Goodenough, J. B., “Phospho-olivines as Positive-electrode Materials for Rechargeable Lithium Batteries”, *J. Electrochem. Soc.*, Vol. 144, No. 4 (1997), pp.1188-1194 .
- (12) Yamada, A., Chung, S. C. and Hinokuma, K., “Optimized LiFePO₄ for Lithium Battery Cathodes”, *J. Electrochem. Soc.*, Vol. 148, No. 3 (2001), pp. A224-A229 .
- (13) Ohzuku, T., Ueda, A. and Yamamoto, N., “Zero-strain Insertion Material of Li[Li_{1/3}Ti_{5/3}]O₄ for Rechargeable Lithium Cells”, *J. Electrochem. Soc.*, Vol. 142, No. 5 (1995), pp. 1431-1435.
- (14) Scharner, S., Weppner, W. and Schmid-Beurmann, P., “Evidence of Two-phase Formation Upon Lithium Insertion into the Li_{1.33}Ti_{1.67}O₄ Spinel”, *J. Electrochem. Soc.*, Vol. 146, No. 10 (1999), pp. 857-861.
- (15) Jiang, J. and Dahn, J. R., “ARC Studies of the Thermal Stability of Three Different Cathode Materials: LiCoO₂; Li[Ni_{0.1}Co_{0.8}Mn_{0.1}]O₂; and LiFePO₄, in LiPF₆ and LiBoB EC/DEC Electrolytes”, *Electrochem. Commun.*, Vol. 6, No. 1 (2004), pp. 39-43.
- (16) Jiang, J., Chen, J. and Dahn, J. R., “Comparison of the Reactions between Li_{7/3}Ti_{5/3}O₄ or LiC₆ and Nonaqueous Solvents or Electrolytes Using Accelerating Rate Calorimetry”, *J. Electrochem. Soc.*, Vol. 151, No. 12 (2004), pp. A2082-A2087.
- (17) Reale, P. et al., “A Safe, Low-cost, and Sustainable Lithium-ion Polymer Battery”, *J. Electrochem. Soc.*, Vol. 151, No. 12 (2004), pp. A2137-A2142.
- (18) Shim, J. and Striebel, K. A., “Effect of Electrode Density on Cycle Performance and Irreversible Capacity Loss for Natural Graphite Anode in Lithium-ion Batteries”, *J. Power Sources*, Vol. 119-121 (2003), pp. 934-937.
- (19) Park, G. et al., “The Study of Electrochemical Properties and Lithium Deposition of Graphite at low Temperature”, *J. Power Sources*, Vol.199 (2012), pp. 293-299.
- (20) Bergveld, H. J. et al., “Adaptive State-of-charge Determination”, *Encyclopedia of Electrochemical Power Sources*, Ed. by Garche, J. (2009), pp. 459-477, Elsevier.
- (21) Ng, K. S. et al., “Enhanced Coulomb Counting Method for Estimating State-of-charge and State-of-health of Lithium-ion batteries”, *Applied Energy*, Vol. 86, No. 9 (2009), pp. 1506-1511.
- (22) He, H. et al., “Online Model-based Estimation of State-of-charge and Open-circuit Voltage of Lithium-ion Batteries in Electric Vehicles”, *Energy*, Vol. 39, No. 1 (2012), pp. 310-318.
- (23) Yazami, R. and Reynier, Y., “Thermodynamics and Crystal Structure Anomalies in Lithium-intercalated Graphite”, *J. Power Sources*, Vol. 153, No. 2 (2006), pp. 312-318.
- (24) Weppner, W. and Huggins, R. A., “Determination of the Kinetic Parameters of Mixed-conducting Electrodes and Application to the System Li₃Sb”, *J. Electrochem. Soc.*, Vol. 124, No. 10 (1977), pp. 1569-1578.
- (25) Striebel, K. et al., “The Development of low cost LiFePO₄-based high Power Lithium-ion Batteries”, *J. Power Sources*, Vol. 146, No. 1-2 (2005), pp. 33-38.
- (26) Guo, X. et al., “The Preparation of LiFePO₄/C Cathode by a Modified Carbon-coated Method”, *J. Electrochem. Soc.*, Vol. 156, No. 10 (2009), pp. A787-A790.
- (27) Joachin, H., Kaun, T. D., Zaghbi, K. and Prakash, J., “Electrochemical and Thermal Studies of LiFePO₄ Cathode in Lithium-ion Cells”, *ECS Trans.*, Vol. 6, No. 25 (2008), pp. 11-16.
- (28) Kao, Y. et al., “Overpotential-dependent Phase Transformation Pathways in Lithium Iron Phosphate Battery Electrodes”, *Chem. Mater.*, Vol. 22, No. 21 (2010), pp. 5845-5855.
- (29) Dreyer, W. et al., “The Thermodynamic Origin of Hysteresis in Insertion Batteries”, *Nature Mater.*, Vol. 9, No. 5 (2010), pp. 448-453.
- (30) Andersson, A. S. and Thomas, J. O., “The Source of First-cycle Capacity Loss in LiFePO₄”, *J. Power Sources*, Vol. 97-98 (2005), pp. 498-502.
- (31) Laffont, L. et al., “Study of the LiFePO₄/FePO₄ Two-phase System by High-resolution Electron Energy Loss Spectroscopy”, *Chem. Mater.*, Vol. 18, No. 23 (2006), pp. 5520-5529.
- (32) Ramana, C. V., Mauger, A., Gendron, F., Julien, C. M. and Zaghbi, K., “Study of the Li-insertion/extraction Process in LiFePO₄/FePO₄”, *J. Power Sources*, Vol. 187, No. 2 (2009), pp. 555-564.
- (33) Delmas, C., Maccario, M., Croguennec, L., Le Cras, F. and Weill, F., “Lithium Deintercalation in LiFePO₄ Nanoparticles via a Domino-cascade Model”, *Nature Mater.*, Vol. 7, No. 8 (2008), pp. 665-671.
- (34) Dreyer, W., Guhlke, C. and Robert, H., “The Behavior of a Many-particle Electrode in a Lithium-ion Battery”, *Physica D*, Vol. 240, No. 12 (2011), pp. 1008-1019.
- (35) Malik, R., Zhou, F. and Ceder, G., “Kinetics of Non-equilibrium Lithium Incorporation in LiFePO₄”,

Nature Mater., Vol. 10, No. 7 (2011), pp. 587-590.

- (36) Gong, Z. and Yang, Y., "Recent Advances in the Research of Polyanion-type Cathode Materials for Li-ion Batteries", *Energy Environ. Sci.*, Vol. 4, No. 9 (2011), pp. 3223-3242.
- (37) Novák, P., Scheifele, W., Joho, F. and Haas, O., "Electrochemical Insertion of Magnesium into Hydrated Vanadium Bronzes", *J. Electrochem. Soc.*, Vol. 142, No. 8 (1995), pp. 2544-2550.
- (38) Kondo, H. et al., "Effects of Mg-substitution in Li (Ni, Co, Al)O₂ Positive Electrode Materials on the Crystal Structure and Battery Performance", *J. Power Sources*, Vol. 174, No. 2 (2007), pp. 1131-1136.

Tsuyoshi Sasaki

Research Fields:

- Batteries and Battery Materials
- Electrochemistry

Academic Degree: Dr.Eng.

Academic Societies:

- The Electrochemical Society
- International Society of Electrochemistry
- The Ceramic Society of Japan
- The Japan Institute of Metals and Materials
- The Electrochemical Society of Japan



Yoshio Ukyo

Research Field:

- Inorganic Materials

Academic Degree: Dr.Eng.

Academic Societies:

- The Ceramic Society of Japan
- The Electrochemical Society of Japan
- The American Ceramic Society
- The Electrochemical Society
- Materials Research Society
- The Society of Powder Technology, Japan

Awards:

- CerSJ Awards for Advancements in Industrial Ceramic Technology, 2002
- Award for Outstanding Papers Published in the Journal of the Ceramic Society of Japan, 2003



Petr Novák*

Research Fields:

- Batteries and Battery Materials
- Interfacial Nonaqueous Electrochemistry
- Development of Electrochemical In-situ (operando) Methods

Academic Degree: Prof. Dr.

Academic Society:

- International Society of Electrochemistry



* Paul Scherrer Institute, Switzerland & ETH Zurich